

OPEN

The freezing Rènyi quantum discord

Xiao-Yu Li¹, Qin-Sheng Zhu^{1,2}, Ming-Zheng Zhu¹, Hao Wu², Shao-Yi Wu² & Min-Chuan Zhu²

As a universal quantum character of quantum correlation, the freezing phenomenon is researched by geometry and quantum discord methods, respectively. In this paper, the properties of Rènyi discord is studied for two independent Dimer System coupled to two correlated Fermi-spin environments under the non-Markovian condition. We further demonstrate that the freezing behaviors still exist for Rènyi discord and study the effects of different parameters on this behaviors.

As an important part of the quantum theory, the quantum correlation has aroused extensive attention in lots of physical fields, such as quantum information^{1–3}, condensed matter physics^{4,5} and gravitation wave⁶ due to some unimaginable properties in a composite quantum system which can not be reproduced by a classical system. In the past twenty years, entanglement was considered as the quantum correlation and gradually understood. But, the quantum discord concept has been put forward by Ollivier and Zurek^{7,8} and Henderson and Vedral⁹ with the deep understanding of quantum correlation. It was clearly demonstrated that entanglement represents only a portion of the quantum correlations and can entirely cover the latter only for a global pure state¹⁰. Later, many efforts have been devoted to quantify quantum correlation from the view of geometry^{10–20} and entropy^{7–9,21–29}.

Since the systematic correlation contains two parts: the classical correlations and quantum correlation, Maziero *et al.*³⁰ found the frozen behavior of the classical correlations for phase-flip, bit-flip, and bit-phase flip channels. As for the possible similar behaviors for the quantum correlation, Mazzola, Piilo, and Maniscalco³¹ displayed the similar behavior of the quantum correlations under the nondissipative-independent-Markovian reservoirs for special choices of the initial state. In the same year, Lang and Caves³² provided a complete geometry picture of the freezing discord phenomenon for Bell-diagonal states. Later, some effort has been devoted to discuss the condition for the frozen-discord with some Non-Markovian processes and initial states^{10,19,20,33} (Bell-diagonal states, X states and SCI atates). In conclusion, the freezing discord shows a robust feature of a family of two-qubit models subject to nondissipative decoherence, that is, the quantum correlation does not change for a while. Although different measures of discords lead to some different conditions for the freezing phenomenon, seeing NMR experiment where the freezing discord was demonstrated³⁴, this phenomenon of quantum correlation reflects a deeper physical interpretation, such as some relationship with quantum phase transition³⁵. Recently, the Rènyi entropy^{36,37}

$$S_{\alpha}(\rho) = \frac{1}{1-\alpha} \log \text{Tr}[\rho^{\alpha}] \quad (1)$$

arouses much attention in the quantum information field. This comes from two aspects: (1) Certain properties of a quantum state ρ which associated to density matrix elements can be quantified in terms of linear or nonlinear functions of ρ , such as the average values $\text{Tr}A\rho$ of observable $\{A\}$ (linear functionals), the von Neumann entropy and the Rènyi entropy (nonlinear functions). Simultaneously, quantum networks can be used to estimate nonlinear functions of ρ more directly and bypass tomography³⁸. (2) The Rènyi entropy shows quantitative bounds for different parameter α comparing the von Neumann entropy, and it is easier to implement than the von Neumann entropy for measuring entanglement^{39–42}. Here the parameter $\alpha \in (0, 1) \cup (1, \infty)$ and the logarithm is in base 2. Notably, the Rènyi entropy will reduce to the von Neumann entropy when $\alpha \rightarrow 1$. As an natural extension of quantum discord, the Rènyi entropy discord (RED)^{36,37,43–45} is also put forward. Therefore, it is valuable to study the properties of RED and the condition for the freezing phenomenon of RED in quantum information field.

¹School of information and software engineering, University of Electronic Science and Technology of China, Chengdu, 610054, P. R. China. ²School of Physics, University of Electronic Science and Technology of China, Chengdu, 610054, P. R. China. Correspondence and requests for materials should be addressed to X.-Y.L. (email: xiaoyu33521@163.com) or Q.-S.Z. (email: zhuqinsheng@gmail.com)

The Quantum Correlation of Dimer System

The definition of Rènyi discord. At first, Ollivier and Zurek^{7,8} gave the concept of quantum discord (QD)

$$D(\rho_{AB}) = \min_{\Pi_k^A} \sum_k p_k S(\rho_k^B) + S(\rho_B) - S(\rho_{AB}) \tag{2}$$

to quantify the quantum correlation, where the von Neumann entropy $S(X) = -tr(\rho_X \log_2 \rho_X)$ is for the density operator ρ_X of system X , $\rho_{A(B)} = Tr_{B(A)}(\rho_{AB})$ is the reduced density matrix by tracing out the degree of the system $B(A)$, $p_k = Tr((\Pi_k^A)^\dagger \rho_{AB} \Pi_k^A)$ and $\rho_k^B = Tr_A((\Pi_k^A)^\dagger \rho_{AB} (\Pi_k^A) / p_k)$. Here, Π_k^A denotes the measurement of system A .

Later, an equivalent description is introduced in refs^{36,37,43,44}. The main idea of this equivalent description is to apply an isometry extension of the measurement map $U_{A \rightarrow EX}$ from A to a composite system EX . This method reveals that any channel from A to A' can be used to describe the composite system EX when we discard the freedom of E . Finally, the quantum discord is rewritten as:

$$D(\rho_{AB}) = \inf_{\Pi_k^A} I(E; B|X)_{\tau_{XEB}} \tag{3}$$

where the optimization is with respect to all possible POVMs Π_k^A of system A with the classical output X . E is an environment for the measurement map and

$$\begin{aligned} \tau_{XEB} &= U_{A \rightarrow EX} \rho_{AB} U_{A \rightarrow EX}^\dagger \\ U_{A \rightarrow EX} |\psi_A\rangle &= \sum_k |k\rangle_X \otimes \left(\sqrt{\Pi_k^A} |\psi_A\rangle \otimes |k\rangle \right)_E \end{aligned} \tag{4}$$

The conditional mutual information $I(E; B|X)_{\tau_{XEB}}$ satisfy:

$$\begin{aligned} I(E; B|X)_{\tau_{XEB}} &= S(\rho_{EX})_{\tau_{XEB}} + S(\rho_{BX})_{\tau_{XEB}} \\ &\quad - S(\rho_X)_{\tau_{XEB}} - S(\rho_{XEB})_{\tau_{XEB}} \end{aligned} \tag{5}$$

where $S(\rho_{EX})$ denotes the von Neumann entropy of the composite system EX for total system EXB which has density matrix τ_{XEB} . Similar definitions for $S(\rho_{BX})$, $S(\rho_X)$ and $S(\rho_{XEB})$.

As an extension of quantum discord, the Rènyi quantum discord of ρ_{AB} is defined for $\alpha \in (0, 1) \cup (1, 2]$ as⁴³

$$D_\alpha(\rho_{AB}) = \inf_{\Pi_k^A} I_\alpha(E; B|X)_{\tau_{XEB}} \tag{6}$$

where the Rènyi conditional mutual information $I_\alpha(E; B|X)_{\tau_{XEB}}$ satisfy:

$$\begin{aligned} I_\alpha(E; B|X)_{\tau_{XEB}} &= \frac{\alpha}{\alpha - 1} \log Tr \left\{ \left(\rho_X^{\frac{\alpha-1}{2}} Tr_E \left\{ \rho_{EX}^{\frac{1-\alpha}{2}} \rho_{EBX}^\alpha \right. \right. \right. \\ &\quad \left. \left. \left. \rho_{EX}^{\frac{1-\alpha}{2}} \right\} \rho_X^{\frac{\alpha-1}{2}} \right)^{\frac{1}{\alpha}} \right\} \end{aligned} \tag{7}$$

In this paper, we choose the von Neumann measurement $\Pi_{i'} = |i'\rangle\langle i'| (i = 0, 1)$ with two angular parameters θ and ϕ : $|0'\rangle = \cos(\theta/2)|0\rangle + e^{i\phi} \sin(\theta/2)|1\rangle$ and $|1'\rangle = \sin(\theta/2)|0\rangle - e^{i\phi} \cos(\theta/2)|1\rangle (0 \leq \theta \leq \pi/2; 0 \leq \phi \leq \pi)$. The properties of the Rènyi quantum discord are shown in Table 2 of ref.⁴³.

The Hamiltonian of the open system. We consider two independent dimer systems which are coupled to two correlated Fermi-spin environments, respectively, as shown in Fig. 1. The Hamiltonian of the total system has the following form⁴⁶:

$$H = H_d + \sum_{i=1,2} H_{B_i} + \sum_{i,j=1,2} H_{d_i B_j} + q S_1^z S_2^z \tag{8}$$

where $H_d = H_{d_1} + H_{d_2}$ and H_{B_i} describe two independent dimer system and Fermi-spin environments, respectively. $H_{d_i B_j}$ represent the interaction between the dimer and the spin environment; while $S_1^z S_2^z$ denotes the interaction between two spin environments. The collective spin operators are defined as $S_i^z = \sum_{k=1}^{N_i} \frac{\sigma_z^{k,i}}{2}$, where $\sigma_z^{k,i}$ are the Pauli matrices and α_i is the frequency of $\sigma_z^{k,i}$. So $q S_1^z S_2^z$ describes an Ising-type correlation between the environments with strength q . The cases $q = 0$ and $q \neq 0$, describe independent and correlated spin bath, respectively. The various parts of the Hamiltonian can be written as following forms:

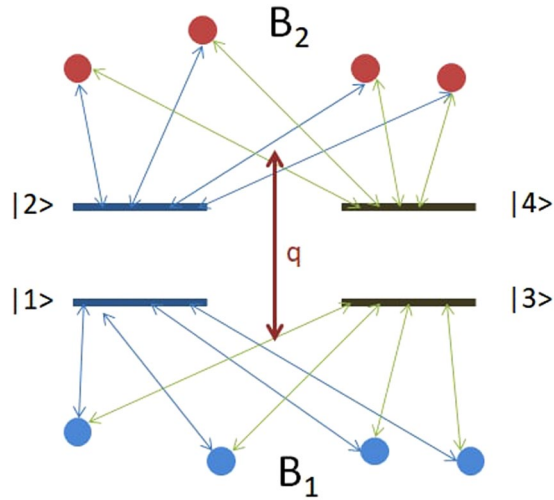


Figure 1. The two dimer systems interacting with two interaction spin-environments (\$S_1\$ and \$S_2\$). The red and blue balls denote the spin particles of environments (\$B_1\$, \$B_2\$), respectively. The \$|1\rangle\$ and \$|2\rangle\$ (\$|3\rangle\$ and \$|4\rangle\$) denote the energy level states of dimer system \$H_{d_1}\$ (\$H_{d_2}\$). \$q\$ denotes the interaction strength between the spin-environments \$S_1\$ and \$S_2\$. The arrows between the energy level states and spin particles of environments denote the interaction between dimer systems and environments.

$$\begin{aligned}
 H_{d_1} &= \varepsilon_1|1\rangle\langle 1| + \varepsilon_2|2\rangle\langle 2| + J_1(|1\rangle\langle 2| + |2\rangle\langle 1|) \\
 H_{d_2} &= \varepsilon_3|3\rangle\langle 3| + \varepsilon_4|4\rangle\langle 4| + J_2(|3\rangle\langle 4| + |4\rangle\langle 3|) \\
 H_{d_1B_1} &= \gamma_1|1\rangle\langle 1|S_1^z; H_{d_1B_2} = \gamma_2|2\rangle\langle 2|S_2^z \\
 H_{d_2B_1} &= \gamma_3|3\rangle\langle 3|S_1^z; H_{d_2B_2} = \gamma_4|4\rangle\langle 4|S_2^z \\
 H_{B_i} &= \alpha_i S_i^z
 \end{aligned}$$

Here, each environment \$B_i\$ consists of \$N_i\$ particles (\$i = 1, 2\$) with spin \$\frac{1}{2}\$; \$\varepsilon_a\$ and \$|a\rangle\$ (\$a = 1, 2, 3, 4\$) are the energy levels and the energy states of the dimer system, \$J_1\$ and \$J_2\$ are the amplitudes of transition. The interaction intensity between the spin particle and the environment is \$\gamma_i\$.

The dynamics evolution of the dimer system. The formal solution of the von Neumann equation (\$\hbar = 1\$)

$$\frac{d}{dt}\rho(t) = \mathcal{L}\rho(t) = -i[H, \rho(t)] \tag{9}$$

can be solved as

$$\rho(t) = e^{\mathcal{L}t}\rho(0) \tag{10}$$

where \$\rho(t)\$ denotes the density matrix of the total system.

The dynamics of the reduced density matrix \$\rho_d(t)\$ is obtained by the partial trace method which discards the freedom of the environments. That is

$$\rho_d(t) = Tr_B(e^{\mathcal{L}t}\rho(0)) \tag{11}$$

Here, the states \$|j, m\rangle\$ denote the orthogonal bases in the environment Hilbert space \$H_B\$ which satisfy⁴⁷:

$$\begin{aligned}
 S^2|j, m\rangle &= j(j+1)|j, m\rangle; \\
 S^z|j, m\rangle &= m|j, m\rangle; S^2 = (S^x)^2 + (S^y)^2 + (S^z)^2 \\
 j &= 0, \dots, \frac{N}{2}; m = j, \dots, -j
 \end{aligned}$$

For the initial state \$\rho(0) = \rho_d(0) \otimes \rho_B(0)\$ condition, the reduced density matrices \$\rho_d(t)\$ of the dimer system is

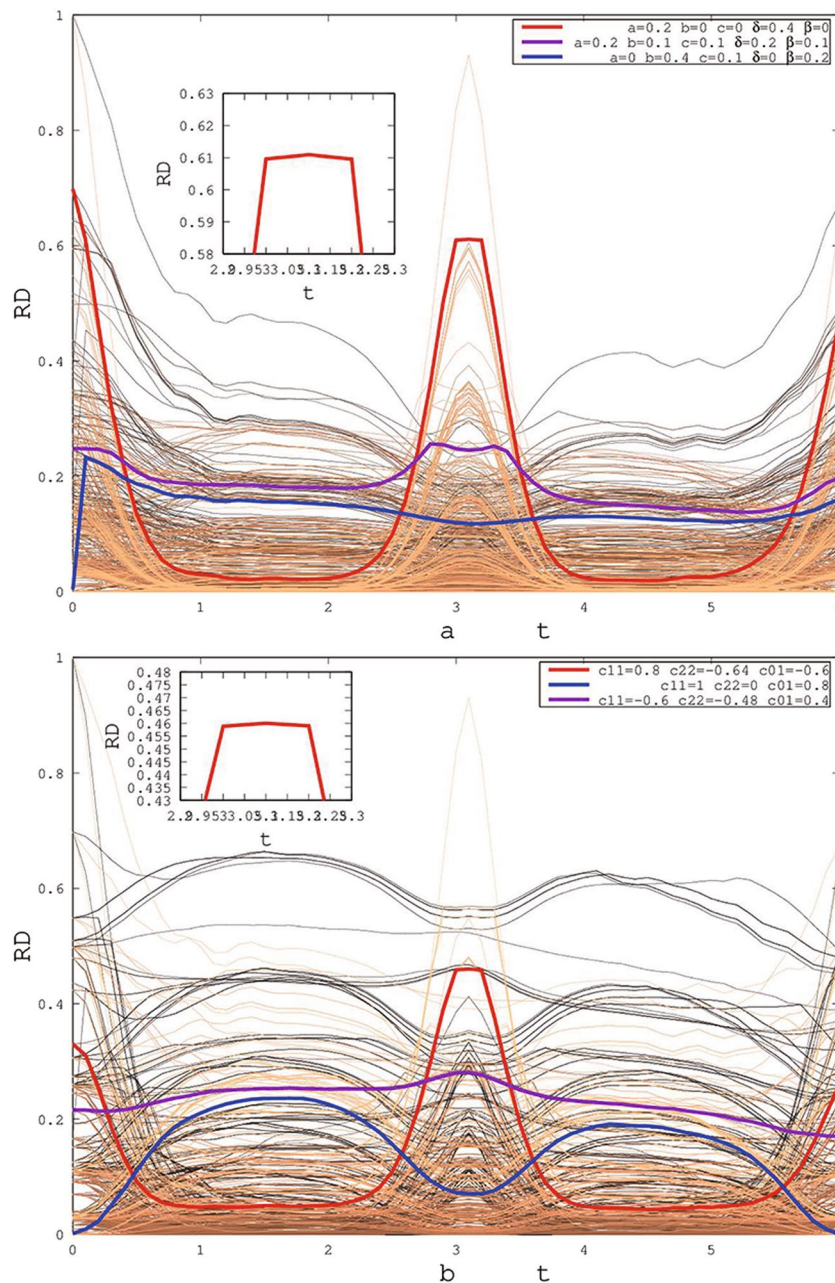


Figure 2. The properties of Rényi discard as a function of time t for X and SCI initial states. The parameters are $\alpha_1 = 250 \text{ ps}^{-1}$, $\alpha_2 = 200 \text{ ps}^{-1}$, $\Delta_1 = 20 \text{ ps}^{-1}$, $\Delta_2 = 10 \text{ ps}^{-1}$, $\Delta_3 = 22 \text{ ps}^{-1}$, $\Delta_4 = 12 \text{ ps}^{-1}$, $q = 30 \text{ ps}^{-1}$, $\beta = 1/77$, $N_1 = 20$, $N_2 = 22$, $\gamma_1 = 1 \text{ ps}^{-1}$, $\gamma_2 = 1.1 \text{ ps}^{-1}$, $\gamma_3 = 0.9 \text{ ps}^{-1}$, $\gamma_4 = 1.2 \text{ ps}^{-1}$, $J_1 = 10 \text{ ps}^{-1}$, $J_2 = 12 \text{ ps}^{-1}$ and $\alpha = 0.9$.

$$\rho_d(t) = \frac{1}{Z} \sum_{j_1=0}^{N_1/2} \sum_{m_1=-j_1}^{j_1} \sum_{j_2=0}^{N_2/2} \sum_{m_2=-j_2}^{j_2} \frac{\nu(N_1, j_1)\nu(N_2, j_2)}{e^{\beta q m_1 m_2} e^{\beta \alpha_1 m_1} e^{\beta \alpha_2 m_2}} \times A^\dagger U^\dagger \rho'_d(0) U A \tag{12}$$

where $\nu(N_i, j_i)$ denotes the degeneracy of the spin bath^{47–49}. $\rho'_d(0)$ is the matrix form of the density operator $\rho_d(0)$ under the basis states of dimer system Hilbert space $A^\dagger = (|3\rangle\langle 1| |3\rangle\langle 2| |4\rangle\langle 1| |4\rangle\langle 2|)$. The symbol U in Eq. (12) denotes the 4×4 matrix and equal to MBQ (here, M, B and Q are also 4×4 matrices⁴⁶).

In order to obtain Eq. (12), the environment is given as the canonical distribution

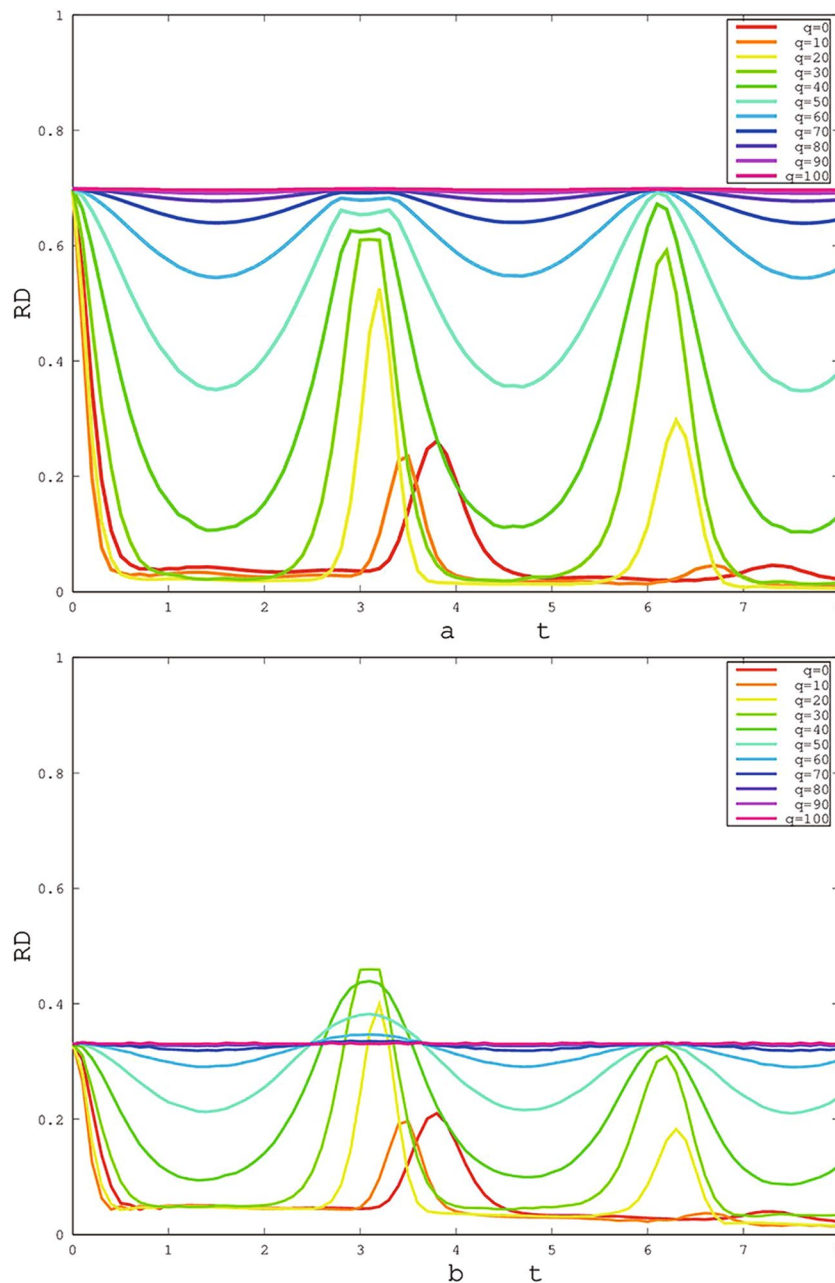


Figure 3. The changes of freezing Rényi discord based on X (a) and SCI (b) initial states (Here, choosing the initial states of red solid line of Fig. 2) with time t for different environment coupling parameters q . The other parameters are same in Fig. 2.

$$\rho_B(0) = \frac{1}{Z} e^{\beta q S_1^z S_2^z} \prod_{i=1}^2 e^{-\beta \alpha_i S_i^z}$$

with $\beta = \frac{1}{K_B T}$ (T is temperature and K_B is Boltzmann constant). The partition function Z is

$$Z = \sum_{j_1=0}^{N_1/2} \sum_{m_1=-j_1}^{j_1} \sum_{j_2=0}^{N_2/2} \sum_{m_2=-j_2}^{j_2} \frac{\nu(N_1, j_1) \nu(N_2, j_2)}{e^{\beta q m_1 m_2} e^{\beta \alpha_1 m_1} e^{\beta \alpha_2 m_2}}$$

The properties of Rényi discord. In this section, the changing behaviors of the quantum correlation are discussed for the two-qubit X¹⁰ and special canonical initial (SCI)³³ under different parameters, respectively. The two-qubit X state is widely used in condensed matter systems and quantum dynamics^{10-12,22,28,29,50-54}. Under the

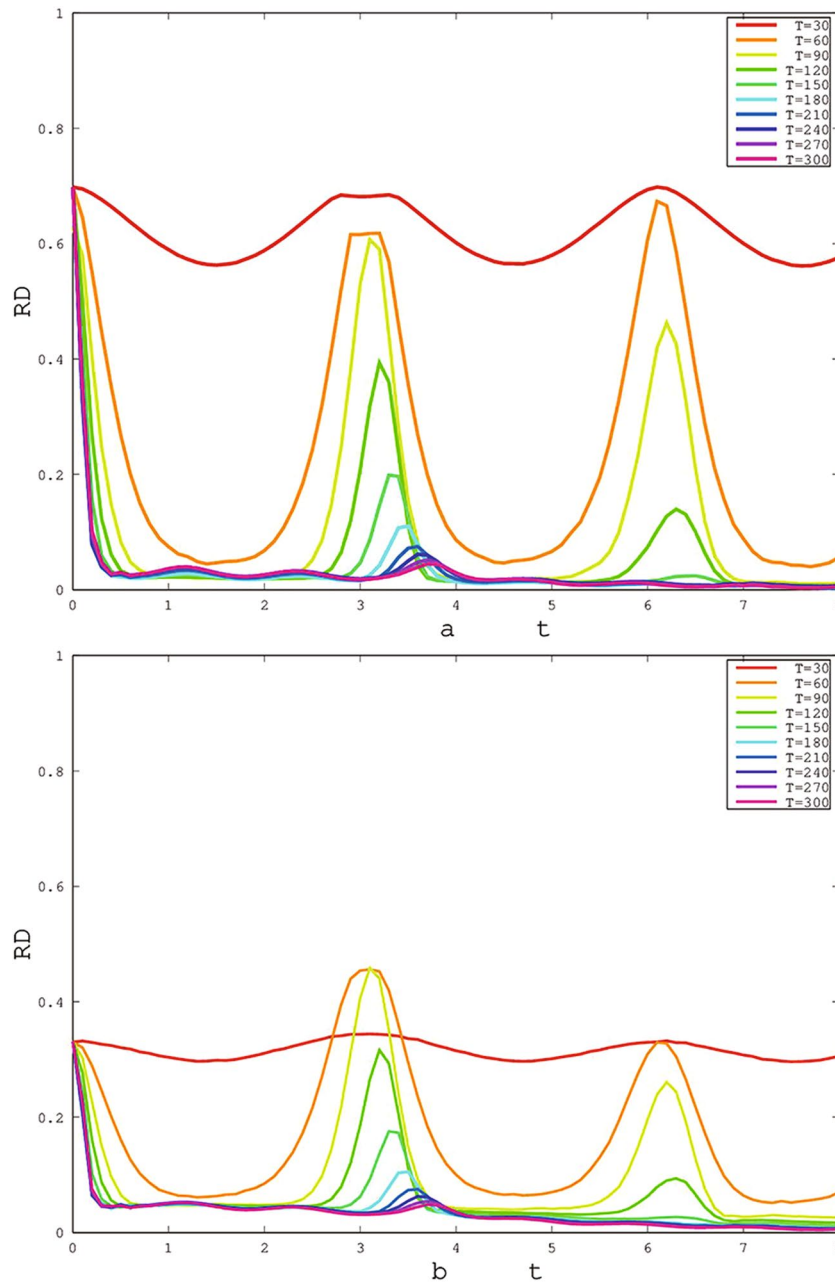


Figure 4. The changes of freezing Rényi discord based on X (a) and SCI (b) initial states (Here, choosing the initial states of red solid line of Fig. 2) with time t for different environment temperatures T . The other parameters are same in Fig. 2.

basis vectors $|00\rangle, |01\rangle, |10\rangle$ and $|11\rangle$ (here 0(1) denotes the spin up (down) state), the density matrix of a two-qubit X state can be written as

$$\rho_d(0) = \begin{bmatrix} a & 0 & 0 & \delta \\ 0 & b & \beta & 0 \\ 0 & \beta^* & c & 0 \\ \delta^* & 0 & 0 & d \end{bmatrix} \tag{13}$$

satisfying $a, b, c, d \geq 0, a + b + c + d = 1, \|\delta\|^2 \leq ad$ and $\|\beta\|^2 \leq bc$.

Unlike X states, the class of canonical initial (CI) states³³ have the density matrix

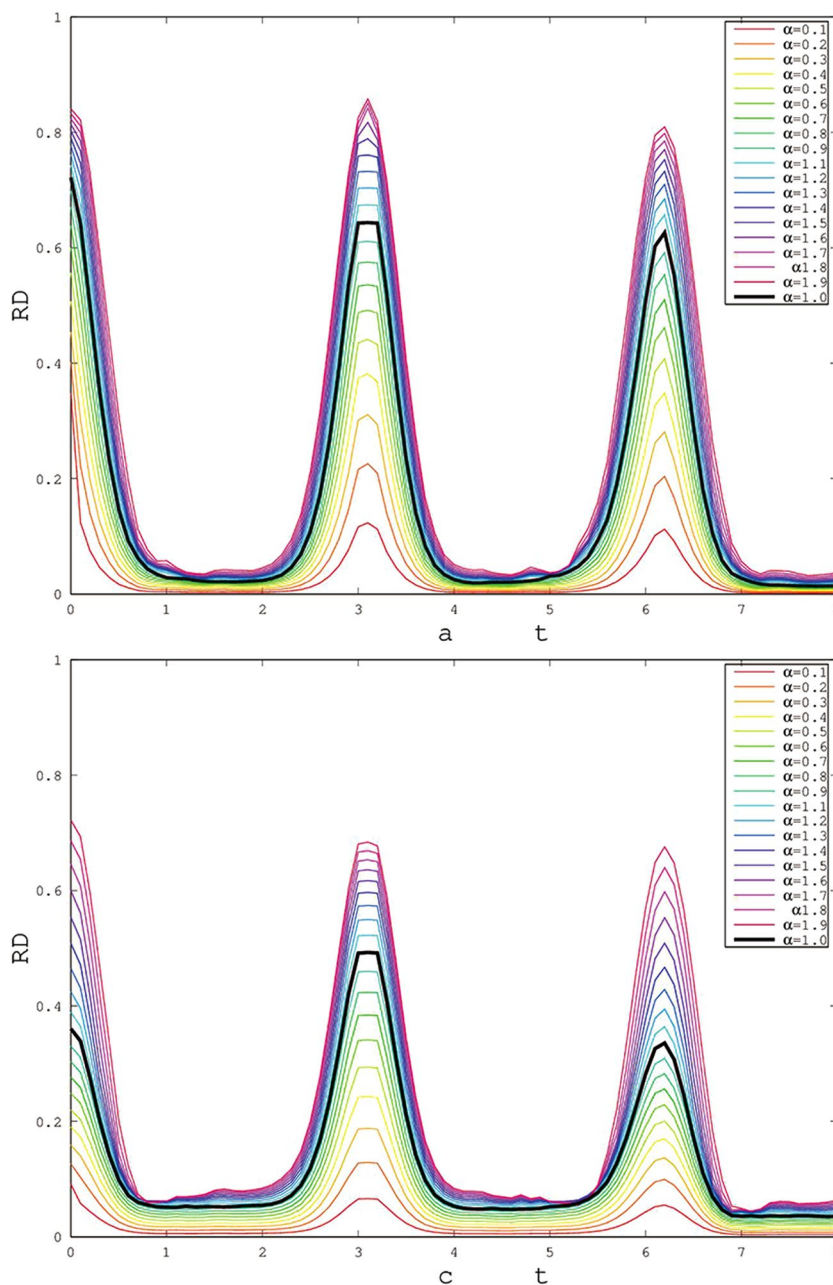


Figure 5. The changes of freezing Rényi discord based on X (Fig. 4(a)) and SCI (Fig. 4(b)) initial states (Here, choosing the initial states of red solid line of Fig. 2) with time t for different parameter α . The other parameters are the same as Fig. 2.

$$\rho_a(0) = \frac{1}{4} \begin{bmatrix} 1 + C_{33} & C_{01} & C_{10} & C_{11} - C_{22} \\ C_{01}^* & 1 - C_{33} & C_{11} + C_{22} & C_{10} \\ C_{10}^* & C_{11} + C_{22} & 1 - C_{33} & C_{01} \\ C_{11} - C_{22} & C_{10}^* & C_{01}^* & 1 + C_{33} \end{bmatrix} \quad (14)$$

and the SCI states satisfy:

$$\begin{cases} C_{22}/C_{33} = -C_{11} \\ C_{10}/C_{01} = C_{11} \\ (C_{33})^2 + (C_{01})^2 \leq 1 \end{cases} \quad (15)$$

In view of the freezing phenomenon for X (SCI) states^{10–12,19,22,28,29,33,50–54} by geometry and von Neumann entropy discords, X and SCI initial states are chosen here.

In Fig. 2, the changing behaviors of quantum correlation are shown for X (Fig. 2(a)) and SCI (Fig. 2(b)) initial states. Every line describes the changing behaviors of quantum correlation for one initial states. With the time evolution, the quantum correlation displays the non-Markov behaviors, especially the peak at about 3 second for some initial states, e.g. red line. It indicates the feedback of quantum information (quantum correlation) with the non-Markov process. When the quantum correlation value fluctuates within the range of 10^{-3} for numerical computation of a computer, we believe that the freezing of quantum correlation occurs. Because there exists the freezing of quantum correlation for some initial states, it is shown quantum correlation of two initial states which exist the freezing phenomenon in Fig. 2. The purple line shows longer freezing phenomenon contrasting with the red line. The red line has larger value of quantum correlation for the freezing platform. It also hints that the freezing phenomenon of quantum correlation is a universal quantum character and has a deep physical meaning. In the inset box, it shows the partially enlarged drawing of the max freezing quantum correlation. Simultaneously, the blue solid line shows the spring of the quantum correlation for the initial states with zero quantum correlation at $t = 0$. It means that we can generate the quantum correlation by the environments of this quantum system. From the physical perspective of information flow, the total correlation of the system changes as the system information flows between the system and the environment, for example, the system information is always lost under the Markov process, and there is the feedback behavior under the non-Markov process. Since the total correlation consists of classical correlation and quantum correlation, in the flow of information, if only the classical correlation changes, then the quantum correlation exists freezing phenomenon.

Although the general results are obtained, the intrinsic parameters may play an important role in the changing behaviors of the quantum correlation^{19,20,21,55}, especially the freezing behavior. In Fig. 3, the environment coupling parameter q can strongly affect the occurrence of freezing phenomenon, and the quantum correlation appears the quasi-periodic oscillations for X (Fig. 3(a)) and SCI (Fig. 3(b)) initial states. However, the oscillation behaviors are depressed with $q \geq 50$ for X and SCI initial states. The freezing phenomena of quantum correlation also spring up with increasing q for X state. But, the freezing phenomena of SCI state first appears with increasing q , and then disappears with $q \geq 70$. Particularly, the freezing phenomena always exist throughout the time when q excesses 90. Furthermore, the value of quantum correlation increases with increasing q for X state. From the perspective of the non-Markovian dynamical process, the larger q means the more information flowing from the system into the environment than that from the environment into the system. Therefore, a reasonable value of q is important for the maintenance of quantum correlation.

Except for the parameter q , the temperature T is also important for the quantum correlation. According to our previous works^{35–37}, a higher temperature may depress the activity of quantum correlation. How does temperature affect the frozen platform? The effect of temperature on the frozen platform is shown in Fig. 4. With increasing temperature T , the frozen platform collapses and then reappears at $T \geq 150$. Simultaneously, the platform height is reduced.

Figure 5 display the effect of different parameters α which is an important parameter of Rènyi entropy for Rènyi discord. With the increase of α , the monotonicity of Rènyi discord is well displayed^{36,37}. For X and SCI initial states, the freezing platform appears in the range of $\alpha \in [0.7, 1.4]$ and $\alpha \in [0.1, 1.6]$, respectively. When the freezing platform appears, there is a particular scope of parameter alpha, which depends on the initial states. It stem from: when we calculate the quantum correlation, the classical correlation is related to the quantification (measurement) method, so the freezing phenomenon is related to the measurement method. Finally, compared the black line ($\alpha = 1$) with others, the quantum discord only shows part of the nature of quantum correlation which quantifies by one of entropy discord, while the others correspond to different entropy discord. This otherness maybe supply the help to discuss the difference between quantum discord and geometric discord, especially, the occurrence of freezing phenomenon has different conditions.

Conclusion

In this paper, the Rènyi discord has been applied to study the properties of quantum correlation of two independent Dimer System which coupled to two correlated Fermi-spin environments for the first time. We also study the freezing behaviors of Rènyi discord for the first time. It show bona fide discord quantification methods all freeze under the certain condition for non-dissipative dynamics and depend on the quantification method (different α) and system parameters, e.g. coupling parameters q and temperatures T . Comparing the quantum discord, the Rènyi discord is more favorable to discuss the upper limit value of the freezing phenomenon and let us understand the robustness of the system.

References

- Nielsen, M. A. & Chuang, I. L. *Quantum Computation and Quantum Information*. (Cambridge University Press, Cambridge, England, 2000).
- Xu, J. Sh. *et al.* Experimental investigation of classical and quantum correlations under decoherence. *Nature Commun* **1**, 7 (2010).
- Xu, J. S. *et al.* Experimental recovery of quantum correlations in absence of system-environment back-action. *Nature Commun* **4**, 2851 (2013).
- Yao, Y. *et al.* Performance of various correlation measures in quantum phase transitions using the quantum renormalization-group method. *Phys. Rev. A* **86**, 042102 (2012).
- Modi, K., Brodutch, A., Cable, H., Paterek, T. & Vedral, V. The classical-quantum boundary for correlations: Discord and related measures. *Rev. Modern Phys* **84**, 1655 (2012).
- Podolskiy, D. & Lanza, R. On decoherence in quantum gravity. *Annalen der physik* **528**, 663 (2016).
- Zurek, W. H. Einselection and Decoherence from an Information Theory Perspective. *Ann. Phys. (Leipzig)* **9**, 855 (2000).
- Ollivier, H. & Zurek, W. H. Quantum Discord: A Measure of the Quantumness of Correlations. *Phys. Rev. Lett.* **88**, 017901 (2001).
- Henderson, L. & Vedral, V. Classical, quantum and total correlations. *J. Phys. A* **34**, 6899 (2001).

10. Cianciaruso, M., Bromley, T. R., Roga, W., Franco, R. L. & Adesso, G. Universal freezing of quantum correlations within the geometric approach. *Sci. Rep* **5**, 10177 (2015).
11. Dakic, B., Vedral, V. & Brukner, C. Necessary and Sufficient Condition for Nonzero Quantum Discord. *Phys. Rev. Lett.* **105**, 190502 (2010).
12. Giampaolo, S. M., Streltsov, A., Roga, W., Bruß, D. & Illuminati, F. Quantifying nonclassicality: Global impact of local unitary evolutions. *Phys. Rev. A* **87**, 012313 (2013).
13. Wootters, W. K. Statistical distance and Hilbert space. *Phys. Rev. D* **23**, 357 (1980).
14. Girolami, D. *et al.* Quantum Discord Determines the Interferometric Power of Quantum States. *Phys. Rev. Lett.* **112**, 210401 (2014).
15. Bera, M. N. Role of quantum correlation in metrology beyond standard quantum limit, arXiv: 1405.5357.
16. Aaronson, B., Franco, R. L., Compagno, G. & Adesso, G. Freezing of quantum correlations under nondissipative decoherence is universal. *New Journal of Physics* **15**, 093022 (2013).
17. Girolami, D., Tufarelli, T. & Adesso, G. Characterizing Nonclassical Correlations via Local Quantum Uncertainty. *Phys. Rev. Lett.* **110**, 240402 (2013).
18. Chang, L. & Luo, S. Remedying the local ancilla problem with geometric discord. *Phys. Rev. A* **87**, 062303 (2013).
19. Ding, C.-C., Zhu, Q.-S., Wu, S.-Y. & Lai, W. The Effect of the Multi-Environment for Quantum Correlation: Geometry Discord vs Quantum Discord. *Annalen der physik* **529**, 1700014 (2017).
20. Zhu, Q., Ding, C., Wu, S. & Lai, W. Geometric measure of quantum correlation: The influence of the asymmetry environments. *Physica A* **458**, 67 (2016).
21. Zhu, Q. S., Ding, C. C., Wu, S. Y. & Lai, W. The role of correlated environments on non-Markovianity and correlations of a two-qubit system. *Eur. Phys. J. D* **69**, 231 (2015).
22. Luo, S. Using measurement-induced disturbance to characterize correlations as classical or quantum. *Phys. Rev. A* **77**, 022301 (2008).
23. Yu, T. & Eberly, J. H. Evolution from entanglement to decoherence of bipartite mixed “X” states. *Quantum Inf. Comput.* **7**, 459 (2007).
24. Chen, Q., Zhang, C., Yu, S., Yi, X. X. & Oh, C. H. Quantum discord of two-qubit X states. *Phys. Rev. A* **84**, 042313 (2011).
25. Lu, X.-M., Ma, J., Xi, Z. & Wang, X. Optimal measurements to access classical correlations of two-qubit states. *Phys. Rev. A* **83**, 012327 (2011).
26. Ali, M., Rau, A. R. P. & Alber, G. Quantum discord for two-qubit X states. *Phys. Rev. A* **81**, 042105 (2010).
27. Ali, M., Rau, A. R. P. & Alber, G. Erratum: Quantum discord for two-qubit X states. *Phys. Rev. A* **82**, 069902(E) (2010).
28. Franco, R. L. *et al.* Dynamics of Quantum Correlations in Two-Qubit Systems Within Non-Markovian Environments. *International Journal of Modern Physics B* **27**, 1245053 (2013).
29. Ma, Z., Chen, Z., Fanchini, F. F. & Fei, S. M. Quantum Discord for $d \otimes 2$ Systems. *Scientific reports* **5**, 10262 (2015).
30. Maziero, J., Céleri, L. C., Serra, R. M. & Vedral, V. Classical and quantum correlations under decoherence. *Phys. Rev. A* **80**, 044102 (2009).
31. Mazzola, L., Piilo, J. & Maniscalco, S. Sudden Transition between Classical and Quantum Decoherence. *Phys. Rev. Lett.* **104**, 200401 (2010).
32. Lang, M. D. & Caves, C. M. Quantum Discord and the Geometry of Bell-Diagonal States. *Phys. Rev. Lett.* **105**, 150501 (2010).
33. Chanda, T., Pal, A. K., Biswas, A., Sen, A. & Sen, U. Freezing of quantum correlations under local decoherence. *Phys. Rev. A* **91**, 062119 (2015).
34. Silva, I. A. *et al.* Observation of time-invariant coherence in a room temperature quantum simulator. *Phys. Rev. Lett.* **117**, 160402 (2016).
35. Yao, Y. *et al.* Performance of various correlation measures in quantum phase transitions using the quantum renormalization-group method. *Phys. Rev. A* **86**, 042102 (2012).
36. Berta, M., Seshadreesan, K. P. & Wilde, M. M. Rényi generalizations of the conditional quantum mutual information. *Journal of Mathematical Physics* **56**, 022205 (2015).
37. Berta, M., Seshadreesan, K. P. & Wilde, M. M. Rényi generalizations of quantum information measures. *Phys. Rev. A* **91**, 022333 (2015).
38. Artur, K. E. *et al.* Direct Estimations of Linear and Nonlinear Functionals of a Quantum State. *Phys. Rev. Lett.* **88**, 217901 (2002).
39. Islam, R. *et al.* Measuring entanglement entropy in a quantum many-body system. *Nature* **528**, 77 (2015).
40. Alves, C. M. & Jaksch, D. Multipartite Entanglement Detection in Bosons. *Phys. Rev. Lett.* **93**, 110501 (2004).
41. Daley, A. J. *et al.* Measuring Entanglement Growth in Quench Dynamics of Bosons in an Optical Lattice. *Phys. Rev. Lett.* **109**, 020505 (2012).
42. Abanin, D. A. & Demler, E. Measuring Entanglement Entropy of a Generic Many-Body System with a Quantum Switch. *Phys. Rev. Lett.* **109**, 020504 (2012).
43. Seshadreesan, K. P., Berta, M. & Wilde, M. M. Rényi squashed entanglement, discord, and relative entropy differences, arXiv:1410.1443.
44. Piani, M. Problem with geometric discord. *Phys. Rev. A* **86**, 034101 (2012).
45. Shaukat, M. I., Slaoui, A., Terças, H. & Daoud, M. Phonon-mediated quantum discord in dark solitons, arXiv:1903.06627 (2019).
46. Zhu, Q.-S., Fu, C.-J. & Lai, W. The Correlated Environments Depress Entanglement Decoherence in the Dimer System. *Z. Naturforsch.* **68a**, 272 (2013).
47. Breuer, H.-P., Burgarth, D. & Petruccione, F. Non-Markovian dynamics in a spin star system: Exact solution and approximation techniques. *Phys. Rev. B* **70**, 045323 (2004).
48. Wesenberg, J. & Molmer, K. Mixed collective states of many spins. *Phys. Rev. A* **65**, 062304 (2002).
49. Hamdouni, Y., Fannes, M. & Petruccione, F. Exact dynamics of a two-qubit system in a spin star environment. *Phys. Rev. B* **73**, 245323 (2006).
50. Benedetti, C., Paris, M. G. A. & Maniscalco, S. Non-Markovianity of colored noisy channels. *Phys. Rev. A* **89**, 012114 (2014).
51. Haikka, P. & Maniscalco, S. Non-Markovian Quantum Probes, <https://arxiv.org/abs/1403.2156>.
52. Rossi, M., Benedetti, C. & Paris, M. G. A. Engineering decoherence for two-qubit systems interacting with a classical environment. *Int. J. Quantum Inf.* **12**, 1560003 (2014).
53. Huang, Y. Quantum discord for two-qubit X states: Analytical formula with very small worst-case error. *Phys. Rev. A* **88**, 014302 (2013).
54. Namkung, M., Chang, J., Shin, J. & Kwon, Y. Revisiting Quantum discord for two-qubit X states: Error bound to Analytical formula, arXiv: 1404.6329 [quant-ph] (2014).
55. Zhu, Q. Sh., Lai, W. & Wu, D. L. Dynamical Symmetry Method Investigates the Dissipation and Decoherence of the two-level Jaynes-Cummings Model. *Z. Naturforsch A* **67a**, 559 (2012).

Acknowledgements

This work was supported by the National Natural Science Foundation of China [61502082] and the Fundamental Research Funds for the Central Universities [ZYGX2014J136].

Author Contributions

X.Y.Li. conceived the model and theoretical calculation. Q.Sh.Zhu. and M.Zh.Zhu. supplied the numerical calculation. H.Wu., S.Y.Wu., and M.C.Zhu. provided comments to the manuscript.

Additional Information

Competing Interests: The authors declare no competing interests.

Publisher's note Springer Nature remains neutral with regard to jurisdictional claims in published maps and institutional affiliations.



Open Access This article is licensed under a Creative Commons Attribution 4.0 International License, which permits use, sharing, adaptation, distribution and reproduction in any medium or format, as long as you give appropriate credit to the original author(s) and the source, provide a link to the Creative Commons license, and indicate if changes were made. The images or other third party material in this article are included in the article's Creative Commons license, unless indicated otherwise in a credit line to the material. If material is not included in the article's Creative Commons license and your intended use is not permitted by statutory regulation or exceeds the permitted use, you will need to obtain permission directly from the copyright holder. To view a copy of this license, visit <http://creativecommons.org/licenses/by/4.0/>.

© The Author(s) 2019